CONTENTS

Experimental Setup

Here we show the details of the experimental setup.

To encode the 2D lattice in time we consider two fiber loops shown in Figure S1(a), labeled up channel and down channel. The length of each fiber loop is ~ 3 (km), and one circulation of light in the loop is equivalent to one step of the walk. Hence, we can encode the entire 2D lattice within a time-duration (or time-delay) of ~ 15000 (ns) without mixing time-bins in step n and step $(n+1)$. As in Figure S1(b), we first encode 30 "Y"-time bins in both the up and down channel, each of time duration 250 (ns) in a total time duration of 7500 (ns). Each "Y"-time bin is then occupied by 30 "X"-time bins, each of time duration 7.5 (ns). At any time, the state of the system is thus represented by a complex vector $(U_{x,y}, D_{x,y})$, encoded in the phase and amplitude of the light pulse circulating in the two fiber loops. We note that in our designed allocation configuration, in particular, the time delay durations, we have chosen shorter delays than in previous 2D synthetic works. This is because, unlike the previously mentioned works where AOMs were used for switching, we have used EOMs which are much faster and can accommodate shorter delays [1, 2].

To initialize the system, we inject a single pulse into the down channel of the fiber loop. We use a continuous wave CW laser with 1550 (nm) wavelength (Optilab DFB-1551-SM-10) and by modulation of this laser using a Thorlabs SOA (SOA1013SXS), we have generated pulses of width ~ 6 (ns) at a repetition rate of 1 (pulse/ms). We then control the polarization of the laser with an inline fiber polarization control (PC) before injecting the light into the down channel with a 90/10 beam splitter. Note that we use two identical 90/10 beam splitters, one for each channel. The 90/10 beam splitter in the down channel is used to inject light into the quantum walk, whereas the 90/10 beam splitter in the up channel is used to weakly couple light pulses out of the quantum walk so that we can measure the pulse power after n steps of evolution using the up channel's PD. Note that the EDFA placed immediately prior to the up channel's PD is merely used to amplify the light pulses coming out of the quantum walk experiment, making it easier for the PD to detect it.

As a pulse enters the system, by default we recognize it as entering the $(x = 0, y = 0)$ time bin, and thus the initial state is $D_{0,0} = 1$. The pulse then sequentially passes through a 50/50 beam splitter denoted as $\pm X$-beam splitter, a pair of time-varying intensity modulators (Optilab IMP-1550-20-PM) is used to impose the correct gain/loss as each time bin (x, y) passes through it, controlled by RF signal generated from Teledyne Lecroy arbitrary waveform generator (T3AWG3252). We then impose a delay of 3 (m) in the up channel and no delay in the down channel. The same procedure then repeats for Y, as shown in Figure S1(a), except the difference in delay between the up and down channels is 100 (m).

To combat photon loss in the walk, we use two Thorlabs erbium-doped fiber amplifiers (EDFA) (EDFA100S), one for each channel. Before amplifying the pulse, we use wavelength division multiplexers (WDM) (DWDM-SM-1-34-L-1-2) to couple a 1543 (nm) CW laser (DFB-1543-SM-30) to the pulses so that the spontaneous emission noise during the amplification is reduced. We decouple the 1550 (nm) pulses from the 1543 (nm) CW laser with the same WDM after the amplification is done. Finally, we use PC to ensure the correct linear polarization for the 1550 (nm) signal pulses. After this, a complete quantum walk step is finished.

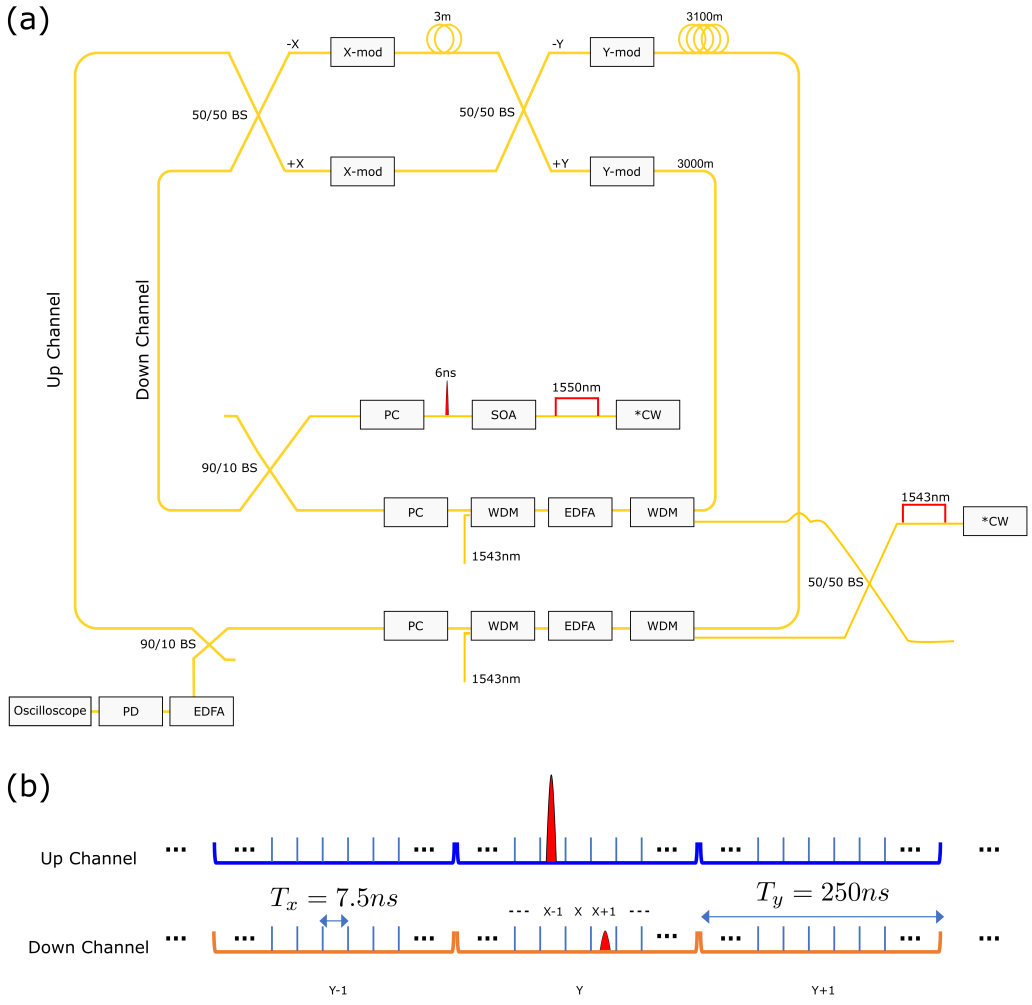

FIG. S1. **Sketch of the complete experimental setup and encoding scheme.** (a) Details of the experiment, with continuous wave (CW) laser, polarization control (PC), wavelength division multiplexer (WDM), photodiode (PD), beam splitter (BS), intensity modulators (X/Y-mod), erbium-doped fiber amplifier (EDFA) and semiconductor optical amplifier (SOA). (b) Encoding the 2D lattice in time bins in two fiber loops. The two loops are named "up channel" and "down channel", respectively.

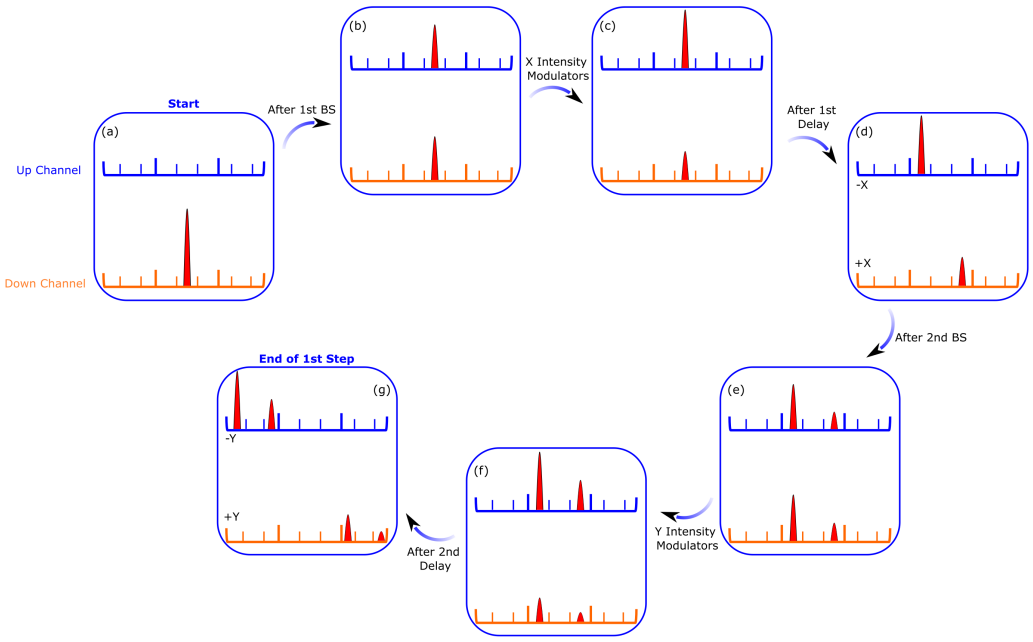

FIG. S2. **Example of full evolution in a complete step.** Both the up and down channels of the fiber loops are shown. (a-g) The complete evolution within one step given that the initial state is $D_{x=0,y=0} = 1$ and all other $U_{x,y}$ and $D_{x,y}$ are 0.

Mathematical formulation of the quantum walk experiment

Here we give the most general mathematical formulation of our quantum walk. Figure S2(a-g) shows this evolution when the input state is $D_{0,0} = 1$.

As mentioned in the previous section, the state at each step is given by a complex vector $(U_{x,y}, D_{x,y})$ where x and y ranges from -15 to $+15$. After the first beam splitter ($\pm X$), the state is updated to (Figure S2(b):

$$\begin{aligned} U^{'}_{x,y} &= \frac{1}{\sqrt{2}}(U_{x,y} - D_{x,y}) \\ D^{'}_{x,y} &= \frac{1}{\sqrt{2}}(U_{x,y} + D_{x,y}) \end{aligned} \tag{S1}$$

After the first pair of modulators ($\pm X$ modulators), we obtain:

$$\begin{aligned} U^{''}_{x,y} &= U^{'}_{x,y} f^{(U)}_{x,y} \\ D^{''}_{x,y} &= D^{'}_{x,y} f^{(D)}_{x,y} \end{aligned} \tag{S2}$$

where $f^{(U/D)}_{x,y}$ is the gain/loss applied to each time bin in the up/down channel by the X modulators.

After the delay:

$$\begin{aligned} U^{'''}_{x,y} &= U^{''}_{x+1,y} \\ D^{'''}_{x,y} &= D^{''}_{x-1,y} \end{aligned} \tag{S3}$$

This yields:

$$\begin{aligned} U^{'''}_{x,y} &= \frac{1}{\sqrt{2}}(U_{x+1,y} - D_{x+1,y}) f^{(U)}_{x+1,y} \\ D^{'''}_{x,y} &= \frac{1}{\sqrt{2}}(U_{x-1,y} + D_{x-1,y}) f^{(D)}_{x-1,y} \end{aligned} \tag{S4}$$

Then, we enter the second beamsplitter ($\pm Y$):

$$\begin{aligned} W^{'}_{x,y} &= \frac{1}{\sqrt{2}}(U^{'''}_{x,y} - D^{'''}_{x,y}) \\ F^{'}_{x,y} &= \frac{1}{\sqrt{2}}(U^{'''}_{x,y} + D^{'''}_{x,y}) \end{aligned} \tag{S5}$$

After modulation ($\pm Y$ modulators):

$$\begin{aligned} W^{''}_{x,y} &= W^{'}_{x,y} c^{(U)}_{x,y} \\ F^{''}_{x,y} &= F^{'}_{x,y} c^{(D)}_{x,y} \end{aligned} \tag{S6}$$

where $c^{(U/D)}_{x,y}$ is the gain/loss applied to each time bin in the up/down channel by the Y modulators.
After delay:

$$\begin{aligned} W^{'''}_{x,y} = W^{''}_{x,y+1} &= \frac{1}{\sqrt{2}}(U^{'''}_{x,y+1} - D^{'''}_{x,y+1}) \times c^{(U)}_{x,y+1} \\ F^{'''}_{x,y} = F^{''}_{x,y-1} &= \frac{1}{\sqrt{2}}(U^{'''}_{x,y-1} + D^{'''}_{x,y-1}) \times c^{(D)}_{x,y-1} \end{aligned} \tag{S7}$$

$(W^{'''}_{x,y}, F^{'''}_{x,y})$ is thus the output state given the input state $(U_{x,y}, D_{x,y})$. Consider a pulse ending up in time bin (x, y) at step $(n+1)$. Denoting it as $U^{(n+1)}_{x,y}$ and $D^{(n+1)}_{x,y}$, we have:

$$\begin{aligned} U^{(n+1)}_{x,y} &= \frac{1}{2}[(U^{(n)}_{x+1,y+1} - D^{(n)}_{x+1,y+1}) f^{(U)}_{x+1,y+1} c^{(U)}_{x+1,y+1} - (U^{(n)}_{x-1,y+1} + D^{(n)}_{x-1,y+1}) f^{(D)}_{x-1,y+1} c^{(U)}_{x-1,y+1}] \\ D^{(n+1)}_{x,y} &= \frac{1}{2}[(U^{(n)}_{x+1,y-1} - D^{(n)}_{x+1,y-1}) f^{(U)}_{x+1,y-1} c^{(D)}_{x+1,y-1} + (U^{(n)}_{x-1,y-1} + D^{(n)}_{x-1,y-1}) f^{(D)}_{x-1,y-1} c^{(D)}_{x-1,y-1}] \end{aligned} \tag{S8}$$

The above equation thus describes the full evolution of the state within one step. We can obtain lattice gain/loss pattern as shown in Figure 1(a) or in Figure 1(c) of the main text, by properly choosing $f^{(U/D)}$ and $c^{(U/D)}$ as a function of (x, y). For example, for a bulk lattice as shown in Figure 1(a) of the main text, we choose $f^{(U)}_{x,y} = \alpha e^{0.175}$, $f^{(D)}_{x,y} = \alpha e^{-0.175}$, $c^{(U)}_{x,y} = \alpha e^{0.175}$, $c^{(D)}_{x,y} = \alpha e^{-0.175}$. Here α is the additional loss imposed by the modulators, and we use EDFA to compensate for the loss such that effectively, $\alpha = 1$. In the experiment, we are only measuring light in the up channel, and thus the power of pulses, or the probability distribution of the walker in the up channel, is

$P_{x,y} \propto |U_{x,y}|^2$. We normalize this probability distribution for all experiment data. Importantly, we also note that while the signal-to-noise ratio is always decreasing as a function of the time step as seen in all the static control measurements, the power intensity distribution in the lattice also changes as a function of the degree of localization of light. This is particularly important in dynamic control over the localization of light at the corner as well as tweezing measurements when the light is localized at the corner after spreading.

Effective band and energy winding of the bulk model

Here we impose periodic boundary conditions for the bulk lattice as shown in Figure 1(a) of the main text, in both X and Y directions. The modulations are $f^{(U)}_{x,y} = e^{0.175}$, $f^{(D)}_{x,y} = e^{-0.175}$, $c^{(U)}_{x,y} = e^{0.175}$, $c^{(D)}_{x,y} = e^{-0.175}$, and thus $\delta_x = 0.175$ and $\delta_y = 0.175$. With this assumption, we can therefore apply the Bloch theorem to the quantum walk evolution equation in the previous section and introduce the Bloch vector (k_x, k_y). We use the ansatz $U_{x,y} = e^{ik_x x + ik_y y}\tilde{U}_{k_x,k_y}$ and $D_{x,y} = e^{ik_x x + ik_y y}\tilde{D}_{k_x,k_y}$ for the eigenmodes of the walk. The evolution equation can now be simplified to:

$$\begin{bmatrix}\tilde{U}_{k_x,k_y}\\ \tilde{D}_{k_x,k_y}\end{bmatrix} = \frac{1}{2}\begin{bmatrix} e^{ik_x+ik_y}f^{(U)}c^{(U)} - e^{-ik_x+ik_y}f^{(D)}c^{(U)} & -e^{ik_x+ik_y}f^{(U)}c^{(U)} - e^{-ik_x+ik_y}f^{(D)}c^{(U)} \\ e^{ik_x-ik_y}f^{(U)}c^{(D)} + e^{-ik_x-ik_y}f^{(D)}c^{(D)} & -e^{ik_x-ik_y}f^{(U)}c^{(D)} + e^{-ik_x-ik_y}f^{(D)}c^{(D)}\end{bmatrix}\begin{bmatrix}\tilde{U}_{k_x,k_y}\\ \tilde{D}_{k_x,k_y}\end{bmatrix} \tag{S9}$$

Since we have two discrete degrees of freedom U and D, we always obtain two different eigenvalues for each (k_x, k_y) as we diagonalize the above 2×2 matrix. We call the two eigenvalues u_{k_x,k_y} and d_{k_x,k_y}. The two effective energies are thus defined as $\epsilon_{up}(k_x, k_y) = ilog(u_{k_x,k_y})$ and $\epsilon_{down}(k_x, k_y) = ilog(d_{k_x,k_y})$.

We further consider the four bulk patches in Figure S3(b) and show that they exhibit different non-Hermitian topological invariants, namely the winding of the effective energy $\epsilon_{up/down}(k_x, k_y)$ in the complex plane. Without loss of generality, we always pick two loops in the Brillouin zone: $l_v = \{k_x \equiv \pi/4, k_y \in [-\pi \to \pi]\}$ and $l_h = \{k_y \equiv \pi/4, k_x \in [-\pi \to \pi]\}$, as shown in Figure S3(a). For each bulk panel in Figure S3(b), as one varies (k_x, k_y) along l_v and l_h, the corresponding complex energy $\epsilon(k_x, k_y)$ can finish a single loop in the complex plane, either in the clockwise or counterclockwise direction. The winding direction of $\epsilon(l_v)$ and $\epsilon(l_h)$ forms the non-Hermitian topological invariant of the bulk. Note that we have suppressed the unimportant label *up* and *down* since $\epsilon_{up}(l_i)$ and $\epsilon_{down}(l_i)$ always wind in the same direction. We note that the formation of corner skin modes in our semi-infinite system is guaranteed by the non-trivial winding in the complex energy plane. In particular, the four domains with different complex hoppings exhibit different directions of winding. At an interface between domains with different windings, we observe skin modes, as shown in Fig.1d in the main text. This phenomenon is similar to that of Hermitian topological systems where two regions with different winding numbers (or topological invariants) show edge modes.

A detailed discussion of the robustness of the corner skin modes is available in Ref. [3].

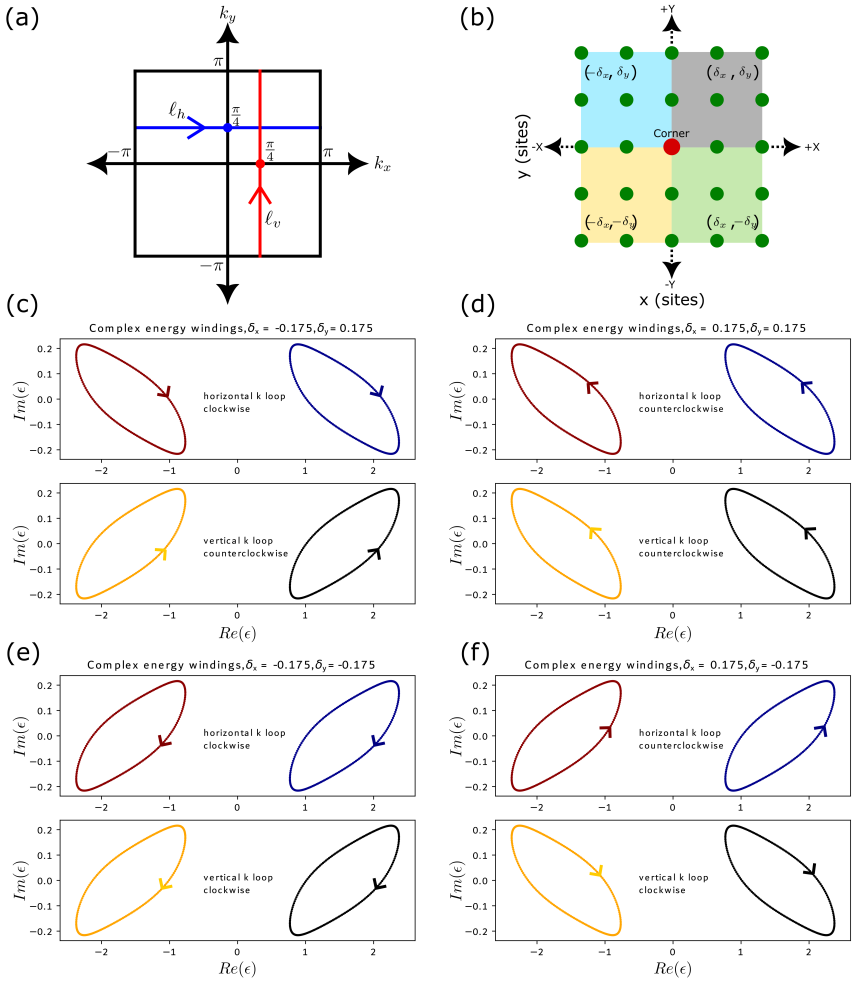

FIG. S3. **Bulk band non-Hermitian topology.** (a) For each bulk patch, we choose two oriented loops in the Brillouin zone: $l_h = \{k_y \equiv \pi/4, k_x \in [-\pi \to \pi]\}$ and $l_v = \{k_x \equiv \pi/4, k_y \in [-\pi \to \pi]\}$. Each loop l_i then contributes to two individual complex energy winding loops $\epsilon_{up}(l_i)$ and $\epsilon_{down}(l_i)$ winding in the same direction. We calculate this winding for all four patches in (b), corresponding to positive or negative δ_x and δ_y. (c-f) The topological invariant is the winding direction of the directed curve $\epsilon(l_h)$ and $\epsilon(l_v)$ in the complex energy plane, which can either be clockwise or counterclockwise.

Localized eigenmodes at the presence of boundary and corner

As shown in Figure 1(d) in the main text, the averaged spatial profile of the eigenmodes of the walk is localized at the corner. In Figure 1(c) of the main text we have chosen $\delta_x = \delta_y = 0.175$, but the feature of the spatial profile persists for any $\delta_x = \delta_y > 0$. Here in Figure S4 of the supplementary section, we show the average eigenmode spatial profile for $\delta_x = \delta_y = 0.03, 0.06, 0.09, 0.12, 0.15$ and 0.18. As one increases $\delta_x = \delta_y$, we observe that the averaged spatial profile becomes more localized.

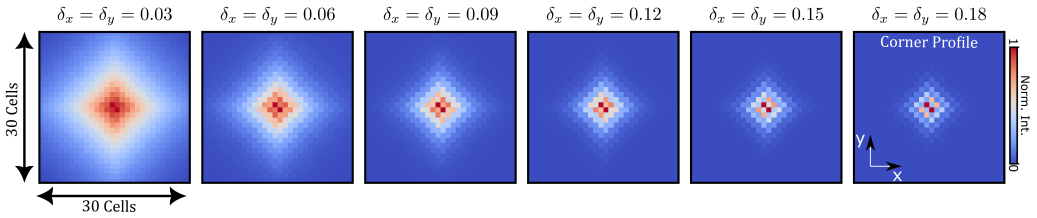

FIG. S4. **Averaged eigenmode spatial profile for different non-Hermitian parameters $\delta_x = \delta_y$.** We adopt the lattice geometry as in Figure S3(b). From left to right we take values $0.03, 0.06, 0.09, 0.12, 0.15$ and 0.18.

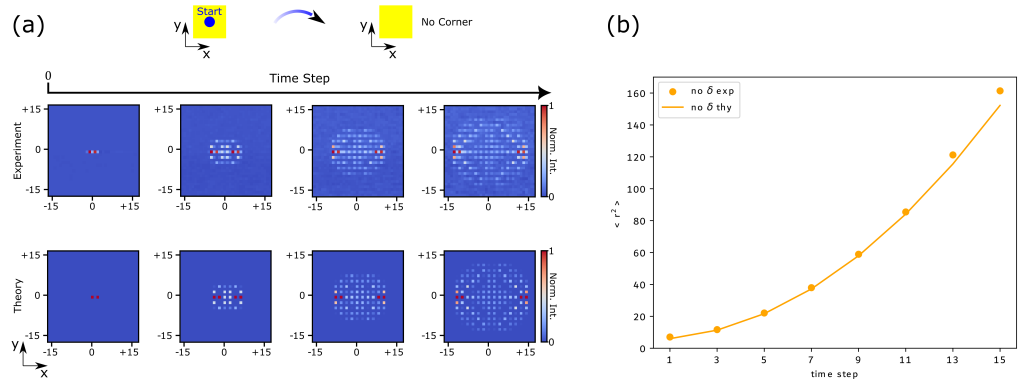

FIG. S5. **Evolution of probability distribution for non-Hermitian parameters $\delta_x = \delta_y = 0$, showing diffusive spreading.** (a) Probability distribution evolution, where the snapshots are taken at time step $1, 5, 9, 13$, respectively. (b) Evolution of averaged displacement $< r^2 >=< x^2 + y^2 >= \sum_{x,y} P_{x,y}(x^2 + y^2)$ for time step from $1, 3, 5, 7, 9, 11, 13$ and 15.

This explains the gradual tapering of the walker's probability distribution as one increases/decreases the non-Hermitian parameter in time, as shown in Figure 3(a) in the main text.

Static control supplementary data

Here we present additional experimental results for the quantum walk with no dynamical control. We first show that, with $\delta_x = \delta_y = 0$, the walker diffusively spreads into the bulk of the lattice, as shown in Figure S5(a), where the probability distribution of the walker is plotted for step $1, 5, 9, 13$. The averaged displacement, defined as $< r^2 > (n) = \sum_{x,y} P_{x,y}(n)(x^2 + y^2)$, is plotted in Figure S5(b), for step $1, 3, 5, 7, 9, 11, 13$ and 15. Here $P_{x,y}$ is the probability distribution of the walker at time step n.

Furthermore, as mentioned in the main text, the funneling of light happens wherever the walker is initialized, assuming the lattice gain-loss pattern shown in Figure 1(c) of the main text. This is manifestly shown in Figure S6, where we always choose the initial state to be $D_{x=0,y=0} = 1$, but lattice corner is located at $(10, -10)$, $(10, 10)$ and $(-10, -10)$, respectively.

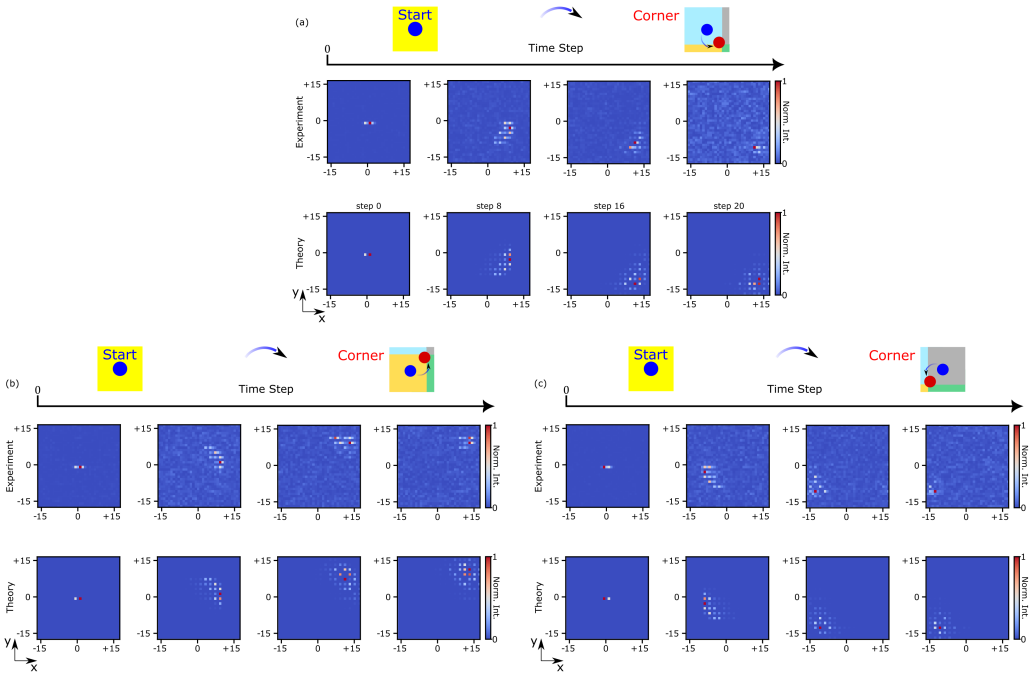

FIG. S6. **Funneling and stabilization of light starting from arbitrary bulk patches.** Light is always initialized at $(x, y) = (0, 0)$, but the corner position is held fixed at (a) $(10, -10)$, (b) $(10, 10)$ and (c) $(-10, -10)$. For each panel, the top row is probability distributions collected at step $1, 9, 17, 21$ of the experiment, and the bottom row is the corresponding simulation results.

[1] A. Schreiber, A. Gábris, P. P. Rohde, K. Laiho, M. Štefaňák, V. Potoček, C. Hamilton, I. Jex, and C. Silberhorn, Science **336**, 55 (2012).

[2] A. L. Muniz, M. Wimmer, A. Bisianov, U. Peschel, R. Morandotti, P. S. Jung, and D. N. Christodoulides, Physical Review Letters **123**, 253903 (2019).

[3] Z. Gong, Y. Ashida, K. Kawabata, K. Takasan, S. Higashikawa, and M. Ueda, Physical Review X **8**, 031079 (2018).